

Article

# Degradation Assessment of Polyethylene-Based Material Through Electrical and Chemical-Physical Analyses

Simone Vincenzo Suraci <sup>1,2,\*</sup>, Davide Fabiani <sup>1</sup>, Laura Mazzocchetti <sup>3</sup> and Loris Giorgini <sup>3</sup>

<sup>1</sup> Laboratory of Innovative Materials for Electrical Systems (LIMES), Department of Electrical, Electronic and Information Engineering, University of Bologna, Viale del Risorgimento 2, 40136 Bologna, Italy; davide.fabiani@unibo.it

<sup>2</sup> PIMM, Arts et Métiers Sciences et Technologies, CNRS, Cnam, HESAM Université, 151 boulevard de l'Hôpital, 75013 Paris, France

<sup>3</sup> Industrial Chemistry Department, University of Bologna, Viale del Risorgimento 4, 40136 Bologna, Italy; laura.mazzocchetti@unibo.it (L.M.); loris.giorgini@unibo.it (L.G.)

\* Correspondence: simone.suraci@unibo.it

Received: 16 January 2020; Accepted: 29 January 2020; Published: 3 February 2020



**Abstract:** The usability of any material hinges upon its stability over time. One of the major concerns, focusing on polymeric materials, is the degradation they face during their service life. The degradation mechanisms are deeply influenced by the aging temperature to which the material is subjected. In this paper, low-density polyethylene (LDPE) flat specimens were thermally aged under two different temperatures (90 °C and 110 °C) and analyzed. Specimens were characterized through both the most common mechanical and chemical measurements techniques (e.g., tensile stress, thermal analyses, oxidation induction time) and electrical measurements (dielectric spectroscopy, in particular), which are examples of non-destructive techniques. As a result, a very spread characterization of the polyethylene-based materials was obtained and a very good correlation was found to exist between these different techniques, highlighting the possibility of following the aging degradation development of polymers through electrical non-destructive techniques.

**Keywords:** low-density polyethylene (LDPE) degradation; thermal aging; dielectric spectroscopy; physical-chemical characterization of polymers; polymer aging; electrical characterization of polymers; polymer thermal analysis; non-destructive testing techniques

## 1. Introduction

Polyethylene-based materials have been widely used as electrical insulation for signal and power cables from low voltage (LV) to high voltage (HV), thanks to their excellent behavior as electrical insulation and high mechanical resistance, and elongation-at-break (EaB), together with enhanced lightness and flexibility. These properties worsen during service mainly due to electric, thermal, and mechanical stresses, as well as environmental factors, like, e.g., humidity, pollution, and UV and gamma radiation. Depending on the final application and on the material formulation, some of these stressors can become the main factors that promote polymer aging. For instance, in electrical engineering applications, electric stress and temperature are the leading aging factors for high voltage (HV) cables, and the main insulation properties are electrical endurance and strength. On the contrary, temperature and mechanical stresses could be predominant for LV cables and, depending on the application, humidity and radiation could also be significant. This latter, particularly gamma radiation, may remarkably affect the cable insulation used in nuclear power plants (NPPs) and aircraft/aerospace applications [1–5]. In general, however, all degradation phenomena occurring in electrical insulation

are strongly regulated by temperature. High temperatures, in fact, can catalyze degradation reactions, above all oxidation, which causes depletion of the material properties [6–10].

In order to prevent premature insulation aging and to provide cable insulation with other functionalities, pure polymers are charged with many different additives, e.g., antioxidants, plasticizers, and flame retardants, which sometimes may exceed 50% of the insulation weight concentration in the case of low voltage cables and indeed undergo their own degradation path [7]. Therefore, low-voltage cable insulation is very often a composite material, whose electric properties depend significantly on the concomitant behavior of all the constituting materials. All these additives contribute, for instance, to hindering the dielectric response, particularly in the low frequency range [1,11–17], thus making the use of electrical measurements at low frequencies to assess the aging state of cable insulating material difficult. This is the reason why aging assessment is almost always based on cable insulation mechanical properties, fixing, e.g., end-of-life at 50% of EaB [18]. It has been shown, however, that aging assessment can be significantly improved by broadening the frequency range of dielectric response measurements [12–16,19]. In the high frequency spectrum of imaginary permittivity, for instance, a good correlation with EaB has been shown in [12] for cables aged under temperature and gamma irradiation. Anyway, the effect of the aging mechanisms, e.g., chain scission, oxidation, and cross-linking, on the dielectric response changes of cable insulation is still not well investigated in the literature. In order to focus the attention on polymer matrix degradation, additives different from antioxidants have been excluded from the study reported in this paper, though they will be considered in future works.

Hence, this paper deals with low-density polyethylene (LDPE) as a precursor for crosslinked polyethylene (XLPE), which is also very commonly used as an electrical insulating polymer for medium voltage and high voltage cables. Accelerated aging was carried out under thermal stress to assess and identify the degradation state of the tested samples by measuring the property change of the samples during aging. LDPE specimens were subjected to two different high temperatures for an appropriate period of time both in air and inert atmosphere to enhance and prevent oxidation, respectively. After aging, polymer specimens were analyzed via chemical, mechanical, and electrical techniques and a correlation among the measured properties was performed.

The aim of this paper was, on the one hand, to widely characterize the degradation development of the aged polymer by the means of different diagnostic techniques, and, on the other hand, to identify the correlation between degradation mechanisms and electrical property changes during aging. This study can provide a step forward for the use of electrical nondestructive techniques to assess the health state of cable insulation.

## 2. Materials and Methods

### 2.1. Specimens

Commercial LDPE tapes were hot pressed through press molding in order to create flat plaques. These latter were then divided into 3 cm × 3 cm area specimens with a thickness of about 200 μm. The hot-pressing parameters are the following:

- Pressure: 2 bars;
- Temperature: 130 °C.

As mentioned in the introduction, polymers for electrical application are filled with different kinds and concentrations of additives. The polymer analyzed in this paper contained only common antioxidants used as stabilizers. However, the type and concentration of antioxidants cannot be disclosed due to a confidentiality agreement with the insulation producer.

### 2.2. Accelerated Aging

Flat specimens were thermally aged in an oven at 90 °C and 110 °C. Differential scanning calorimetry (DSC) showed that these two temperatures are respectively slightly lower and higher

than the polymer melting temperature range, hence, very different behaviors of the polymer with aging were evaluated. Regarding 90 °C aging, the maximum treatment time reached was 1000 h and sampling was made every 200 h.

On the contrary, specimens thermally treated at 110 °C were aged both in air and in inert atmosphere (nitrogen), in order to highlight and neglect the oxidation contribution during thermal stress, respectively. Sampling was made every 300 h and the maximum aging time was 1500 h.

### 2.3. Experimental Setup

#### 2.3.1. Electrical Measurements

Electrical properties, in particular the complex permittivity as a function of the frequency, were investigated by means of the dielectric spectroscopy technique obtained through a Novocontrol Alpha Dielectric analyzer.

The complex permittivity is described by the following formula:

$$\hat{\epsilon} = \epsilon' - j\epsilon'',$$

where  $\epsilon'$  is the real part of permittivity defined as the dielectric constant of the material, and  $\epsilon''$  is the imaginary part of permittivity related to the dielectric losses of the material [8,11,12,16].

The instrumentation was set with the following test parameters:

- Applied voltage: 3 V<sub>rms</sub>;
- Frequency range: 10<sup>-2</sup>–10<sup>6</sup> Hz
- Temperature: Room temperature (~25 °C).

#### 2.3.2. Mechanical Measurements

Tensile tests were carried out at room temperature with a universal tensile testing machine (REMET TC10) equipped with a 100 N load cell, using a crosshead speed of 20 mm/min and initial gauge length of 20 mm. At least four different specimens were tested for each batch (different ageing times and atmosphere). In particular, Elongation-at-break (EaB) was evaluated since it is used, as stated above, in standards [18] as a requested condition for the qualification of LV cable insulations.

#### 2.3.3. OIT\* Measurements

Oxidation induction time (OIT) was evaluated via a TA Instruments STD SQ600 device capable of simultaneously performing differential scanning calorimetry (DSC) and thermogravimetric analysis (TGA) measurements. Due to the actual experimental setup, air was used as the testing atmosphere instead of pure oxygen [20], so that the numerical values reported here refer to air induction to oxidation, labelled as OIT\*. OIT\* tests are quantitative measurements of the polymer tendency to oxidation, and, in general, the lower the OIT\*, the higher the oxidisability grade. OIT measurements were carried out using open alumina pans, both for the sample and the reference, with heating in an inert atmosphere (nitrogen: 100 mL/min gas flow) rapidly (20 °C/min) to the temperature at which the OIT value was determined, which in the present case was 200 °C. When the temperature was reached, the sample was left in isotherm for 5 min, then the atmosphere gas was switched to air (100 mL/min gas flow), and the measurement was kept isothermally for as long as the heat flow signal recorded in DSC mode displayed an exothermic trend, which can be referred to as the oxidation processes. Usually, 10–20 min of air isotherm time was required to conclude the test. Each test was run at least twice to provide reliable results.

#### 2.3.4. Crosslinking Grade Measurements

Gel fraction measurements were performed as requested by standards [21] in xylene in order to evaluate the crosslinking grade. The sample specimen was cut in an appropriate dimension so that their

weight was comparable (about 0.4/0.5 g). They were exactly weighed on an analytical balance (accurate to 0.0001 g) to provide the initial mass ( $M_i$ ) and each of them was placed in a 250-mL round-bottomed flask equipped with a condenser and magnetic stirrer. Then, 100 mL of xylene were added and the mixture was heated at 110 °C for 24 h, after which the samples were removed from the solvent and allowed to dry at room temperature (RT) for 24 h in a desiccator. When samples were dried, they were weighed with an analytical balance to obtain the final gelled mass ( $M_g$ ):

$$\text{Crosslinking grade (\%)} = \frac{M_g}{M_i} 100. \quad (1)$$

### 2.3.5. FTIR Measurements

A Bruker with ALPHA's Platinum ATR single reflection diamond ATR module was used to perform Fourier transform infrared (FTIR) spectroscopy, as reported in Figure 4. Spectra were recorded with a 32 scan acquisition and 4 cm<sup>-1</sup> spectral resolution in the 4000–400 cm<sup>-1</sup> window.

## 3. Results and Discussion

In the present work LDPE was crosslinked in the melting state, a common process to obtain an electrical insulating material for medium voltage and high voltage cables. In this context, interchain reactions are promoted in the melt and to a reasonably low extent. It has indeed been proven that the formation of cross-link junctions in the melt amorphous phase hampers the reorganization and chain folding that leads to crystallization, without completing preventing them, and this results in the formation of a smaller amount of imperfect crystallites with a smaller size [22]. The final product is more of a gel than a hard thermoset. While it is no longer able to dissolve and melt, the polymer becomes a flexible network and not a hard and rigid material either, since the latter condition would be detrimental for the performance of the cable. The long linear segments are thus still able to rearrange in a crystal phase upon cooling. Such a modification is usually perceived as a lowering of the melting temperature from 110–115 °C down to 95–105 °C. From this observation, the two annealing temperatures, at 90 °C and 110 °C, were selected. While these temperatures are close to the melting of the system, the presence of cross-linking prevents the film from losing its shape and dimension during the ageing tests.

### 3.1. Results

Figure 1 shows the trend of the real (Figure 1a,c,e) and imaginary (Figure 1b,d,f) part of permittivity as a function of the frequency for different aging conditions and periods. Generally speaking, as expected, both the real and imaginary part of permittivity increase with the raising of the aging period due to the thermal degradation that occurs inside the polymer.

For the 90 °C aging (Figure 1a,b), the real part shows an almost flat trend in the high frequency range and an increase with the lowering of the frequency. During aging,  $\epsilon'$  shows an initial significant increase during the first aging period while longer periods causes very little variations with aging.

On the contrary, the imaginary part of permittivity has a plane trend in the whole frequency range analyzed here, so that no polarization peak can be highlighted, as expected for a very low-filled polymer. Here, again, the biggest increase is shown to occur during the first aging period. Then, the increase is smaller but constant, so that the whole aging treatment response is placed in the same order of magnitude (Figure 1b).

The 110 °C in-air aging (Figure 1c,d) causes a wider variation of  $\epsilon'$  with aging time with respect to the in-nitrogen treatment due to the different degradation phenomena that occur. In particular, referring to the real part of permittivity (Figure 1c), very small differences with aging time can be seen for the first 900 h of aging; 1200 h of aging, in fact, causes an increase of  $\epsilon'$  in the very low-frequency range imputable to both quasi-DC conduction (Q-DC) [8,17] and electrode polarization. This latter phenomenon can be explained through the presence of free ions inside the polymer, which tend

to move towards the electrode/sample interface, leading to the development of ionic double layers. Electrode polarization (EP) depends microscopically upon the electrode surface topography and area, as well as upon the surface chemistry (reactive surface groups or atoms) [8]. Longer aging periods (1500 h) result in a huge raise of the real part of permittivity (up to 6.9) due to enhanced polarization phenomena, lower values of  $\epsilon'$  in the high frequency range can be imputed to the Q-DC, and the electrode polarization peak just discussed.

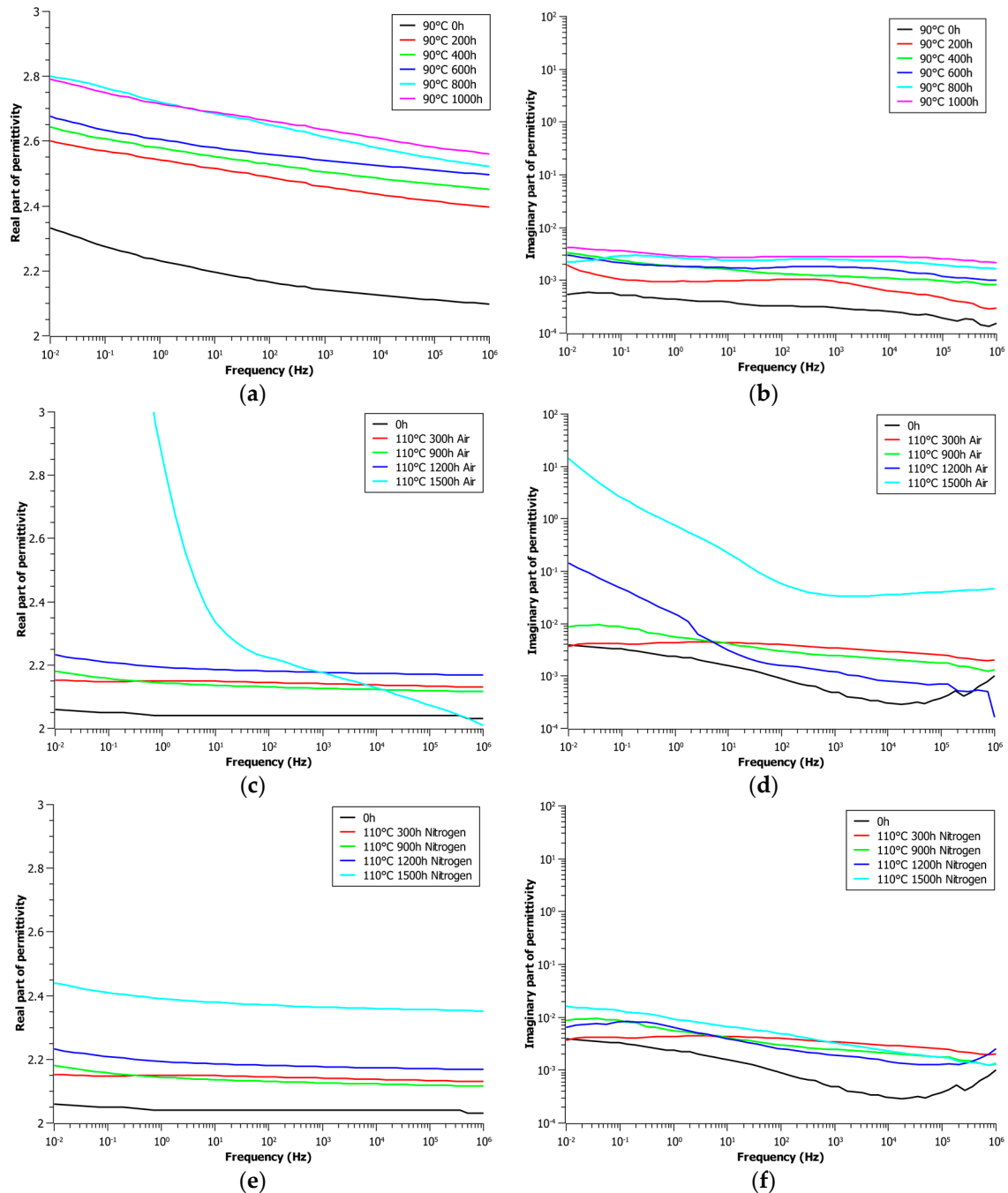


**Figure 1.** Real (a,c,e) and imaginary (b,d,f) part of permittivity as a function of the frequencies and aging times of 90 °C in air, 110 °C in air, and in nitrogen aging, respectively.

Focusing on the imaginary part of permittivity for the 110 °C aging (Figure 1d,f), the first aging period leads to an increase of almost one order of magnitude of the dielectric losses, probably due to the enhanced aging temperature in both the aging conditions analyzed. In air, a gradual raise of  $\epsilon''$

values with aging time can be noticed in the first 1200 h of aging at low frequencies, while slightly no differences can be appreciated in the other frequency ranges. Further aging causes a huge increase of dielectric losses in the whole dielectric spectra up to two orders of magnitude due to very harsh degradation of the specimen induced by thermal aging. It is worth noting that in the low-frequency range,  $\epsilon''$  shows a slope of  $-1$ , which is showed in the literature [8] to be related to the already discussed Q-DC phenomena.

Aging in inert atmosphere (nitrogen) was carried out in order to neglect the contribution of oxidation during the aging process (Figure 1e,f). As a result, the real part of permittivity shows almost no variation with aging until 1200 h of treatment; the longer period (1500 h) causes a considerable increase probably due to the very important degradation state of the sample.

After the first aging period, the imaginary part of permittivity (Figure 1f) does not appreciably change with aging time, so that its trend lines are almost overlapped, suggesting that dielectric losses stay stable during aging in an inert atmosphere.

Referring to mechanical behavior, EaB results are reported in Figure 2. In all the conditions considered, EaB decreases in comparison to the non-aged material, as expected. In particular, the 90 °C aging trend shows an initial significant decrease during the first aging time (by 15%), while further aging causes almost negligible changes. These little differences can be imputed to specimen measurement uncertainty.

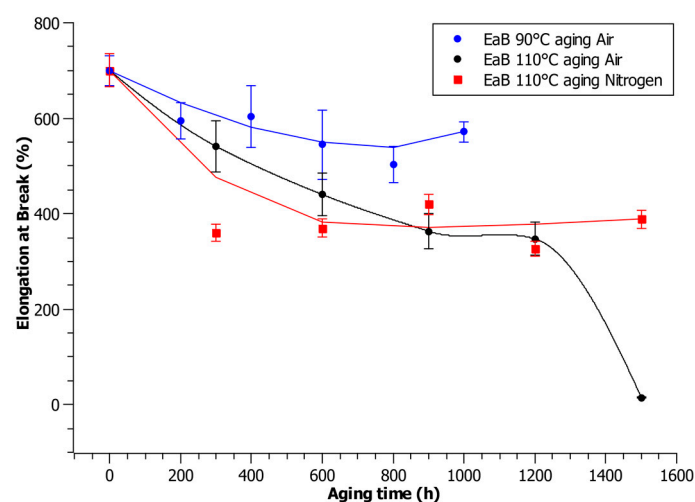


**Figure 2.** Elongation-at-break value as a function of aging time at 90 and 110 °C.

The elongation-at-break results for the 110 °C aging and for both the conditions considered show that the first aging period causes a significant decrease of the EaB value. In particular, the in-air treatment causes a constant decrease of EaB, which results in an abrupt reduction of the relative EaB (under 50%) for very long aging periods (longer than 1200 h).

On the contrary, the in-nitrogen treatment causes very little changes of the EaB value after the first aging period, which can be imputed to specimen-related measurement uncertainty so that the EaB value can be considered as constant during the whole aging period considered here and no important mechanical modification occurs.

Predictably, the oxidation induction time value of the same aging condition (Figure 3) decreases with the increase of the aging time. In fact, thermally activated aging catalyzes thermo-oxidative reactions whose radicals react with antioxidants fillers. As a result, gradual antioxidant consumption leads to a decrease of the OIT\* value.

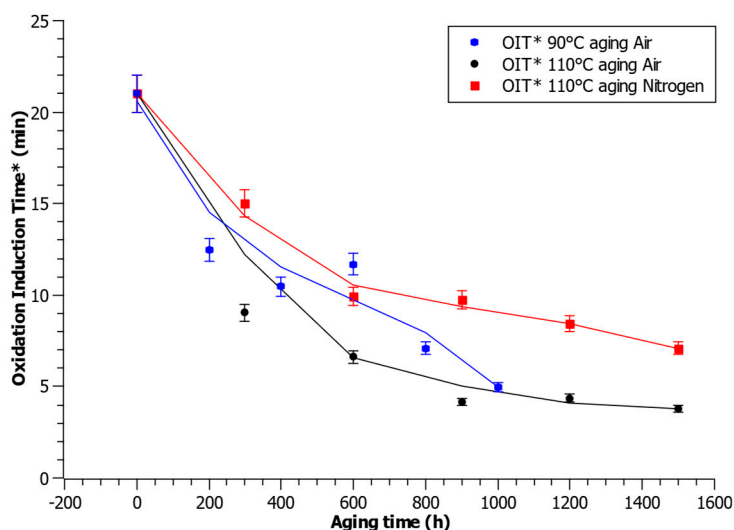


Figure 3. OIT\* measurements as a function of aging time a 90 °C and 110 °C.

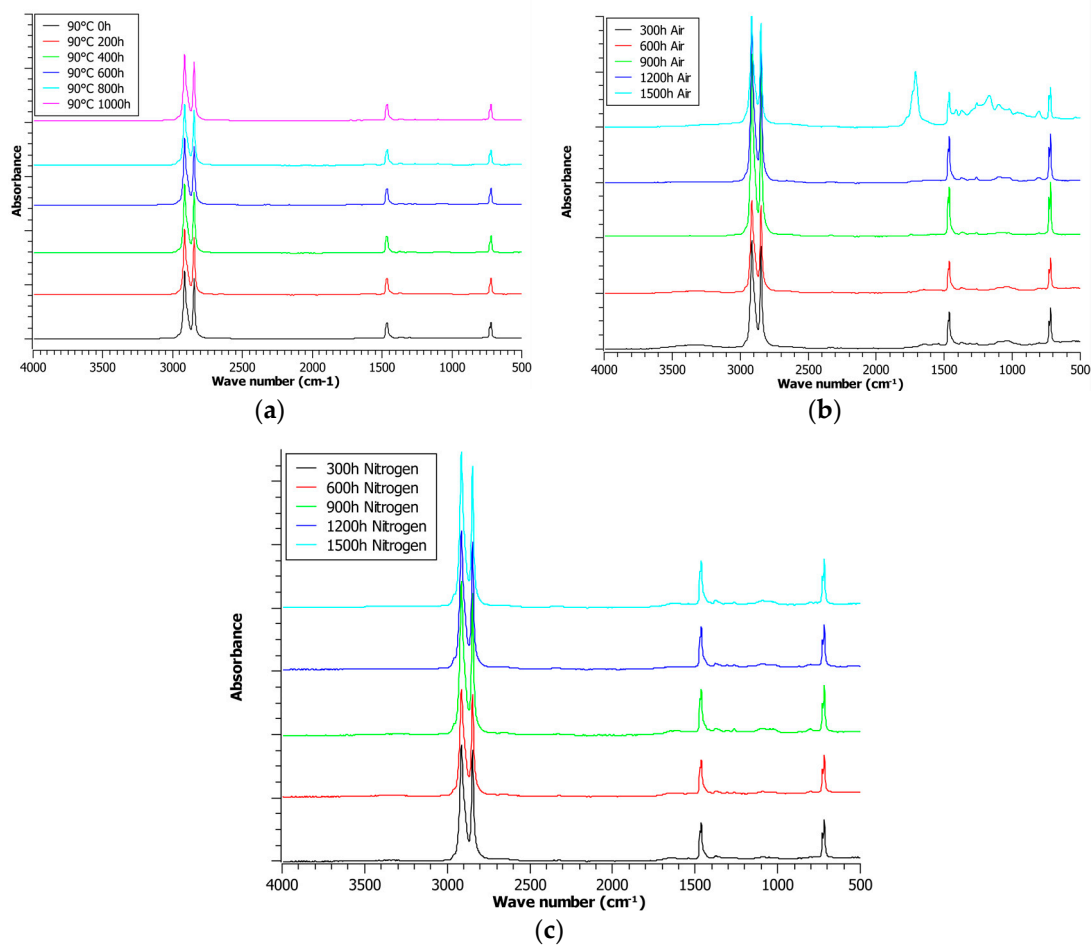
In particular, in-air aging leads to a more substantial decrease of the OIT\* value with respect to the nitrogen treatment imputable to antioxidant depletion made by environmental oxygen, which induces a reduction, by about 25%, from the initial OIT\* value.

Figure 4 shows the FT-IR measurements performed on the flat 90 °C and 110 °C aged samples. It is worth noting that basically no difference, referring to the 90 °C aging, can be appreciated among the spectra of the differently aged specimens, suggesting that no external functional group increased during aging.

Focusing on the 110 °C aging, it is worth commenting that the first 600 h of in-air aging causes no significant alteration to the infra-red spectra of the aged samples, while further ageing up to 1200 h leads to minor variations on the FT-IR spectra, with a slight increase in absorptions ranging in the 835–800  $\text{cm}^{-1}$  and 1400–1000  $\text{cm}^{-1}$  region, typical of C–O bonds. The lack of a signal typical of C = O moieties can be taken as a signal that in the initial stages of the degradation, only hydroxyl, ether, and epoxy groups were formed. On the contrary, the 1500 h aged specimen shows significant peak differences in the above cited regions together with an intense absorption peak in the spectrum around 1700  $\text{cm}^{-1}$  ascribed to carbonyl and carboxyl functional groups [23].

In nitrogen, the FT-IR spectra keep the same trend for the whole aging period investigated here, suggesting that no oxidative group was formed during the treatment, as expected.

Figure 5 reports the trend of the crosslinking grade with aging time for the 110 °C aging. As expected, the crosslinking grade increases linearly with aging, in particular, in-air aging causes wider variation of the crosslinking percentage than in nitrogen due to the effects of thermo-oxidative reactions, as will be discussed hereafter.



**Figure 4.** FT-IR measurements for different aging time in air (a) 90 °C aging; (b) 110 °C aging, and in nitrogen (c) 110 °C aging.

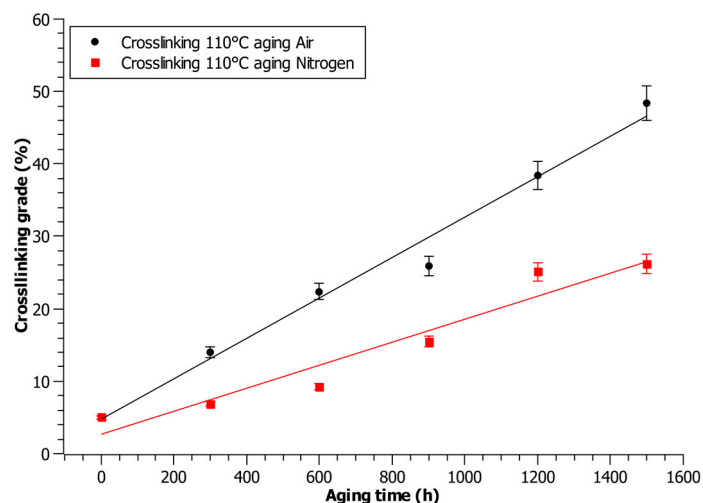


**Figure 5.** Crosslinking grade as a function of the aging time: (black) in air; (red) in nitrogen 110 °C aging.

### 3.2. Discussion

Since the imaginary part of permittivity is the factor related to dielectric losses [8,11,12,16], one can claim that, as expected, in all the aging conditions analyzed here, the losses increase with the increase of the aging time, which is a symptom of the polymer degradation process. In this case, LDPE

degradation provokes a progressive and constant raise in the  $\epsilon''$  value, and it can likely be attributed to additives, in particular antioxidants, gradual consumption, as confirmed by OIT\* measurements (Figure 3) [20], and the creation of antioxidant products during aging.

As known in the literature [8], antioxidants are used as stabilizers for polymer blends rather than as oxidation prevention additives; however, during the aging process, a huge part of the antioxidants is consumed by thermo-oxidative reactions. As discussed above, the OIT\* value is a marker of the oxidisability of polymer blends [20]. Consequently, it is often used as a marker of antioxidant consumption so that the lower the OIT\* value, the lower the antioxidant efficiency and concentration.

In particular, for 90 °C aging, OIT\* linearly decreases during aging, as shown in Figure 3. However, longer aging periods are needed in order to induce oxidation, since OIT\* keeps quite a high value also after 1000 h of aging. This prevents the spread of thermo-oxidative reactions and, consequently, the formation of oxidative groups, as confirmed by FT-IR measurements (Figure 4), which do not show any oxidation-related peak. Contextually, the dielectric spectroscopy measurements show a slight increase of the complex permittivity. In particular, the dielectric losses do not show enhanced variation during aging (Figure 1b), confirming the abovementioned initial stage of degradation.

A higher temperature (110 °C) and longer treatment period (1500 h) induced significant modifications in the polymer physical and chemical properties, which also lead to wider changes in the dielectric spectra (Figure 1). Indeed, the literature reports for polyethylene a degradation pathway that is more prominent in amorphous regions and whose rate is strongly dependent on the oxygen diffusion within the polymer bulk [24]. The raise in the ageing temperature from 90 to 110 °C is a significant change in terms of the LDPE bulk properties [25], since the crystalline aggregates are mostly removed and the polymer will thus be more prone to all the thermo-oxidative processes that pave the way to a dramatic degradation [26]. However, it is worth pointing out that while the polymeric chain might be affected, degradation occurs via random chain scission. This process is not easily macroscopically detected at the very initial stages, since an effective mass loss will be observed only at far higher temperatures above 250 °C [24]. Finally, this condition might also allow for an easier migration of the antioxidants towards the surface, where most of the initial degradation might occur.

Again, both the real and imaginary parts of permittivity show a raise of their value with aging. In both the aging conditions analyzed, the dielectric loss ( $\epsilon''$ ) values are about an order of magnitude higher than that of the 90 °C aging, suggesting an enhancement of the aging process with higher temperature, as expected. In air, the  $\epsilon''$  (Figure 1b,d) raise is likely imputed to progressive additive consumption as reported in the literature [19] and stated above. This is also confirmed by the chemical tests performed and, especially, it can be related to the reduction of the OIT\* value as discussed.

After the complete depletion of the additives, in particular antioxidants, which are the only ones considered here, the thermal treatment causes a huge increase in the whole spectra of up to two orders of magnitude (1500 h aging time). Various authors [11–13] claim that the raise of  $\epsilon''$  in the high frequency range of the spectrum ( $10^5$ – $10^6$  Hz) may be caused by dipolar peaks, which appear in higher frequencies (e.g.,  $10^6$ – $10^9$  Hz) [8,11–13]. The theoretical basis of this lies on the fact that oxygen is a strong dipolar molecule, which, once bonded with radicals, may create dipolar species, causing the raise of the  $\epsilon''$  value. The experimental data, with the appearance, in the FT-IR measurements, of some signal in the  $1400$ – $100$   $\text{cm}^{-1}$  as well as the  $835$ – $800$   $\text{cm}^{-1}$  spectral regions, suggests that in the preliminary steps of the degradation, only single C-O-containing moieties form, such as hydroxyl, ether, and epoxy groups. The strong presence of oxidative groups in the 1500 h aged sample is also reported in the FT-IR spectrum (Figure 4b), which shows peaks related to the carbonyl and carboxyl functional groups ( $1700$   $\text{cm}^{-1}$ ).

This polymer behavior with aging can be related to one of the elongations at breaks reported in Figure 2. EaB in air, in fact, tends to decrease with the increase of the aging time, but the aging period longer than 1200 h brings about an abrupt decrease of EaB. This probably due to some preliminary random chain scission, which slightly diminishes the entanglement ability of the macromolecular chains, thus leading to some minor loss in the ultimate properties at break, without dramatically

affecting the overall mechanical performance: This fact compared well with the FT-IR findings. Indeed, when the FT-IR spectrum shows a strong change in the chemical composition, a drop in EaB is observed: Very low EaB values, indeed, result in very poor mechanical properties, such as an absolute EaB value lower than 50%.

The imaginary part of permittivity in nitrogen (Figure 1f) shows a negligible increase with aging, which may be caused by the very low additive consumption caused by the thermal treatment in the applied conditions. In agreement, no important changes in the polymer properties with aging can be seen in the chemical and mechanical tests. In fact, the EaB values (Figure 2) for this aging condition stay stable for the whole aging process, confirming a strong correlation between polymer degradation, oxidation, and the depletion of mechanical properties.

Moreover, the OIT\* (Figure 3) and crosslinking grade (Figure 5) measurements show linear and slow variations with aging time. As expected, the in-air treatment causes a larger decrease of OIT\* with the aging time and higher increase of the crosslinking grade due to thermo-oxidative reactions, which reduce the concentration of antioxidants and increase the oxidisability of the polymer blend. In the same way, aging in nitrogen causes a reduction of OIT\* and a raise of the crosslinking grade; however, the variation is lower and only imputable to the thermal effect of aging, e.g., radical formation, which can lead to molecular rearrangement and embrittlement of the polymer. The cross-linking effect, which cannot be easily detected by FT-IR spectroscopy since no significant chemical modification to the composition occurs (i.e., polar O-containing moieties formation), is a direct consequence of the antioxidant depletion, as observed via the OIT\* decrease. Indeed, when no more protection comes from the additive, radicals are able to form, and they are not active just towards the oxygen-involving reaction. In this case, the ageing atmosphere mainly affects the additive depletion (that is more rapid in air than in nitrogen), which in turn allows the radical to form just because of the thermal conditions.

As presented, the various characterization techniques analyzed here have related each other, claiming the possibility of performing a quantitative analysis from the chemical microscale characteristics and the electrical macroscale ones in a framework of a multiscale analysis.

To do so, a correlation among these various properties was performed. In particular, a relationship between the high frequency dielectric response and the total esters absorbance peaks obtained by the FT-IR spectra is possible and was shown to be consistent in previous works [12,27]. Unfortunately, since the material analyzed here shows no ester peak in the base material (lack of external antioxidants, e.g., phenol-based molecules), the total absorbance peak (Figure 4) is almost zero and the dielectric losses (Figure 1d) in the high frequency region show very little variation with aging (inside the same order of magnitude) until the last aging period (1500 h) in air. As a point of fact, the 1500 h aging in air period shows a huge increase of the dielectric losses (Figure 1d) and a significant ester peak increase in the FT-IR measurements (Figure 4), suggesting a correlation between these two parameters. This could be explained considering the polar properties of the ester groups [12], as previously discussed.

Moreover, a tentative correlation between the low frequency dielectric response and the crosslinking grade can be highlighted in Figure 5. As a result, the dielectric permittivity at low frequencies was shown to be related to the increase of the crosslinking grade with aging time. Indeed, for both the aging conditions considered (in air and under nitrogen), there is an exponential dependence between these two parameters, as shown in Figure 6. This behavior could be linked to the fact that the crosslinked moieties reveal reduced mobility under the electric field; therefore, its dielectric relaxation time is longer in comparison to non-crosslinked moieties. This corresponds to an increase of the low-frequency dielectric losses probably due to a lower frequency polarization peak out of the analyzed range. It is worth commenting that the longest nitrogen aging shows no significant increase of the crosslinking grade (less than 30%). As a result, the imaginary part of permittivity remains in the same order of magnitude for the entire aging period and no exponential raise can be observed.

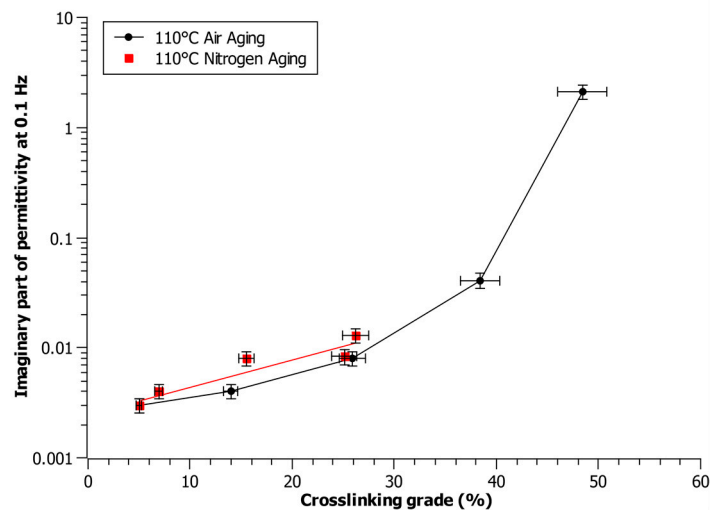


**Figure 6.** Crosslinking grade as a function of the imaginary part of permittivity at 0.1 Hz for 110 °C in air and under nitrogen aging.

#### 4. Conclusions

This research focused on the change of the physical-chemical properties of low-density polyethylene (LDPE) with thermal aging. In particular, the choice of two different aging temperatures, slightly lower and higher than the start of the melting area, as investigated via DSC, lead to a spread analysis of the thermal degradation of the analyzed polymer. In particular, the low temperature aging treatment provoked no substantial degradation of the insulated material so that both the electrical and physical-chemical tests showed very little modification of the polymer characteristics. On the contrary, higher temperature aging brought about an important degradation state, which led to larger variation in the polymer properties. Moreover, the aging process in both air and nitrogen allowed the investigation of oxygen role during the aging process. It was highlighted, in fact, that in-air aging causes very significant modifications of the physical-chemical properties due to the presence of oxygen, which is, as known and discussed, the keystone of the thermo-oxidative reactions and, consequently, of the degradation.

In addition, this work allowed the correlation between degradation mechanisms and changes in dielectric spectroscopy to be identified, this appeared to be a good non-destructive technique for an investigation of the degradation of polymeric matter.

In this sense, this research can be considered the first step for the setup of a condition monitoring technique based on dielectric spectroscopy, which could lead to the building of standards for cable qualification based on non-destructive electrical techniques.

**Author Contributions:** Conceptualization, D.F., L.G., L.M. and S.V.S.; methodology, D.F., S.V.S. and L.M.; formal analysis, S.V.S. and L.M.; investigation, S.V.S.; resources, D.F. and L.G.; data curation, S.V.S. and L.M.; writing—original draft preparation, S.V.S. and L.M.; writing—review and editing, S.V.S., D.F. and L.M.; supervision, D.F. and L.G.; All authors have read and agreed to the published version of the manuscript.

**Funding:** This research received no external funding.

**Acknowledgments:** Authors are grateful to Vittorio Maceratesi, Stefano Bulzaga, Emanuele Spaolonzi and Stefano Merighi for performing the tests.

**Conflicts of Interest:** The authors declare no conflict of interest.

#### References

1. Assink, R.A.; Gillen, K.T.; Bernstein, R. *Nuclear Energy Plant Optimization (NEPO) Final Report on Aging and Condition Monitoring of Low-Voltage Cable Materials*; Office of Scientific and Technical Information (OSTI): Oak Ridge, TN, USA, 2005.

2. IAEA. *Assessing and Managing Cable Ageing in Nuclear Power Plants*; International Atomic Energy Agency: Vienna, Austria, 2012.
3. Celina, M.; Linde, E.; Brunson, D.; Quintana, A.; Giron, N. Overview of accelerated aging and polymer degradation kinetics for combined radiation-thermal environments. *Polym. Degrad. Stab.* **2019**, *166*, 353–378. [[CrossRef](#)]
4. Celina, M.C. Review of polymer oxidation and its relationship with materials performance and lifetime prediction. *Polym. Degrad. Stab.* **2013**, *98*, 2419–2429. [[CrossRef](#)]
5. Simmons, K.L.; Jones, A.M.; Fifield, L.S.; Prowant, M.; Westman, M.P.; Pardini, A.F.; Tedeschi, J.R.; Ramuhalli, P. *Determining Remaining Useful Life of Aging Cables in Nuclear Power Plants—Interim Status for FY2014*; PNNL: Richland, WA, USA, 2014.
6. Wang, Z.; Wei, R.; Ning, X.; Xie, T.; Wang, J. Thermal degradation properties of LDPE insulation for new and aged fine wires. *J. Therm. Anal. Calorim.* **2019**, *137*, 461–471. [[CrossRef](#)]
7. Bartsch, N.; Girard, M.; Wilde, A.; Bruhn, T.; Kappenstein, O.; Vieth, B.; Hutzler, C.; Luch, A. Thermal Stability of Polymer Additives: Comparison of Decomposition Models Including Oxidative Pyrolysis. *J. Vinyl Addit. Technol.* **2018**, *25*, E12–E27. [[CrossRef](#)]
8. Menczel, J.D.; Prime, R.B. *Thermal Analysis of Polymers: Fundamentals and Applications*; Wiley & Sons: New York, NY, USA, 2009.
9. Da Cruz, M.; Van Schoors, L.; Benzarti, K.; Colin, X. Thermo-oxidative degradation of additive free polyethylene. Part I. Analysis of chemical modifications at molecular and macromolecular scales. *J. Appl. Polym. Sci.* **2016**, *133*. [[CrossRef](#)]
10. Courvoisier, E.; Bicaba, Y.; Colin, X. Multi-scale and multi-technical analysis of the thermal degradation of poly(ether imide). *Polym. Degrad. Stab.* **2018**, *147*, 177–186. [[CrossRef](#)]
11. Jonscher, A.K. Dielectric relaxation in solids. *J. Phys. D Appl. Phys.* **1999**, *32*, R57–R70. [[CrossRef](#)]
12. Linde, E.; Verardi, L.; Fabiani, D.; Gedde, U. Dielectric spectroscopy as a condition monitoring technique for cable insulation based on crosslinked polyethylene. *Polym. Test.* **2015**, *44*, 135–142. [[CrossRef](#)]
13. Bowler, N.; Liu, S. Aging Mechanisms and Monitoring of Cable Polymers. *Int. J. Prog. Health Manag.* **2015**, *6*, 1–12.
14. Kim, C.; Jin, Z.; Jiang, P.; Zhu, Z.; Wang, G. Investigation of dielectric behavior of thermally aged XLPE cable in the high-frequency range. *Polym. Test.* **2006**, *25*, 553–561. [[CrossRef](#)]
15. Verardi, L.; Fabiani, D.; Montanari, G.C. Correlation of electrical and mechanical properties in accelerated aging of LV nuclear power plant cables. In Proceedings of the 2014 ICHVE International Conference on High Voltage Engineering and Application, Institute of Electrical and Electronics Engineers (IEEE), Poznan, Poland, 8–11 September 2014; pp. 1–4.
16. Suraci, S.V.; Fabiani, D.; Li, C. Additives effect on dielectric spectra of crosslinked polyethylene (XLPE) used in nuclear power plants. In Proceedings of the 2019 IEEE 37th Electrical Insulation Conference (EIC), Calgary, AB, Canada, 16–19 June 2019; pp. 410–413.
17. Liu, T.; Fothergill, J.; Dodd, S.; Nilsson, U. Dielectric spectroscopy measurements on very low loss cross-linked polyethylene power cables. *J. Phys. Conf. Ser.* **2009**, *183*, 012002. [[CrossRef](#)]
18. Standard IEC/IEEE 62582-3. *Nuclear Power Plants—Instrumentation and Control Important to Safety—Electrical Equipment Condition Monitoring Methods—Part 3: Elongation at Break*; Nuclear Power Engineering Committee: Buffalo, NY, USA, 2012.
19. Suraci, S.V.; Fabiani, D.; Mazzocchetti, L.; Maceratesi, V.; Merighi, S. Investigation on Thermal Degradation Phenomena on Low Density Polyethylene (LDPE) through Dielectric Spectroscopy. In Proceedings of the 2018 IEEE Conference on Electrical Insulation and Dielectric Phenomena (CEIDP), Cancun, Mexico, 21–24 October 2018; pp. 434–437.
20. Schmid, M.; Affolter, S. Interlaboratory tests on polymers by differential scanning calorimetry (DSC): Determination and comparison of oxidation induction time (OIT) and oxidation induction temperature (OIT\*). *Polym. Test.* **2003**, *22*, 419–428. [[CrossRef](#)]
21. ASTM D2765. *Standard Test Methods for Determination of Gel Content and Swell Ratio of Crosslinked Ethylene Plastics*; ASTM International: West Conshohocken, PA, USA, 2016.
22. Liu, S.-Q.; Gong, W.-G.; Zheng, B.-C. The Effect of Peroxide Cross-Linking on the Properties of Low-Density Polyethylene. *J. Macromol. Sci. B* **2014**, *53*, 67–77. [[CrossRef](#)]

23. Silverstein, R.M.; Webster, F.X.; Kiemle, D.J. Infrared Spectrometry. In *Spectrometric Identification of Organic Compounds*, 8th ed.; Wiley & Sons: New York, NY, USA, 2014.
24. Bolbukh, Y.; Kuzema, P.; Tertykh, V.; Laguta, I. Thermal degradation of polyethylene containing antioxidant and hydrophilic/hydrophobic silica. *J. Therm. Anal. Calorim.* **2008**, *94*, 727–736. [[CrossRef](#)]
25. Butler, T.I. PE Processes. In *Multilayer Flexible Packaging*; William Andrew Publishing: Norwich, NY, USA, 2010; pp. 15–30.
26. Abdou, S.M.; Elnahas, H.H.; El-Zahed, H.; Abdeldaym, A. Thermal behavior of gamma-irradiated low-density polyethylene/paraffin wax blend. *Radiat. Eff. Defects Solids* **2016**, *171*, 1–8. [[CrossRef](#)]
27. Suraci, S.V.; Fabiani, D.; Li, C.; Xu, A.; Roland, S.; Colin, X. Aging assessment of XLPE LV cables used in nuclear power plants. In Proceedings of the 10th International Conference on Insulated Power Cables, Paris Versailles, France, 23–27 June 2019.



© 2020 by the authors. Licensee MDPI, Basel, Switzerland. This article is an open access article distributed under the terms and conditions of the Creative Commons Attribution (CC BY) license (<http://creativecommons.org/licenses/by/4.0/>).